Electronic Stability Control for Powered Two-Wheelers

Pierpaolo De Filippi, Mara Tanelli, *Senior Member, IEEE*, Matteo Corno,
Sergio M. Savaresi, *Senior Member, IEEE*, and Mario D. Santucci

I. Introduction and Motivation

ELECTRONIC control systems are present in all commercial cars. Anti-lock braking systems (ABS) and traction control (TC) are employed to improve performance and safety in acceleration and braking maneuvers [1], [2], while electronic stability control (ESC) systems actively modify the vehicle dynamics in order to restore vehicle stability in the face of dangerous maneuvers, [3]–[5].

The development of active control systems for powered two-wheelers (PTW) has started with a significant time delay. This is due to economic, cultural, and technical factors. Namely, the PTW market is limited and the amount of investments on R&D is also limited. Moreover, many riders believe that they do not need any help riding their bikes and that electronic control systems alter the riding experience. Finally, and most interesting from an engineering point of view, dealing with motorcycle dynamics is more complex than it is for four-wheeled vehicles (see [6], [7]). Only in recent times, motorcycle manufactures have started working on production versions of traction control systems, ABS and slow-adaptive control of steering dampers, [8]–[10].

In the scientific literature, some preliminary results have been obtained that address the control of PTW. The problem of controlling the traction of motorcycles is addressed in [11] and [12]. The design of braking control systems is addressed in [13] and [14]. Moreover, some interesting results have also been obtained with semi-active control strategies: in [15] and [16], an industrially amenable control strategy to damp the weave and wobble modes by acting on a semi-active steering damper was proposed. In [17], burst oscillations are suppressed with a mechanical steering compensator. In [18], cornering weave oscillations are reduced controlling the geometry of the rear suspension. In [19], the control of an autonomous motorcycle using the steering torque and the wheel angular velocity as control parameters is presented.

The stability control is the most challenging and complex problem when dealing with PTWs and it is still a fully open research topic. In fact, the experience on four-wheeled vehicles cannot be directly reused because of the coupling between in-plane and out-of-plane modes [20]. This paper is based on the preliminary results presented in [21] and [22], and to the best of our knowledge, constitutes the first attempt to address the active stability control of PTWs.

To put the work into perspective, it is worth noting that the roadmap to arriving at an industrial product that is mainly constituted of a new control system is made up of three different steps. The first is a detailed feasibility study, aimed at formalizing the control problem and proving whether investments in the considered direction are worth or not. Second, once the potential of the new application has been ascertained in selected simulation tests, an extensive simulation campaign must be conducted, which combines all conditions that make sense for the practical application. In motorcycles, in fact, experimental testing is much more complicated for four-wheeled vehicles, due to the necessary safety measures that must be considered for the professional riders who perform the tests. If the simulation campaign also yields favorable results, then one moves to the real vehicle, and fine tuning of the control algorithm takes place. This paper reports the results of the first and part of the second step of the aforementioned roadmap, and it is, therefore, certainly subject to further analyses and improvements in each of the aspects involved. However, it has the merit of presenting a new application, and possibly giving rise to a new research line in motorcycle control. Furthermore, the results are encouraging, proving that there is space for new approaches and new solutions, for which the one proposed herein may serve as a benchmark. This goal is pursued by first presenting an analysis of the motorcycle dynamics in cornering conditions, and investigating the possible and most suitable controlled variables for stability control. Based on this, a control strategy that increases the stability of the motorcycle while taking into account the rider's commands are presented. It is assumed that the motorcycle is equipped with ride-by-wire actuators, i.e.,

Manuscript received November 22, 2012; accepted December 6, 2012. Manuscript received in final form January 4, 2013. Date of publication February 1, 2013; date of current version December 17, 2013. This work was supported by MIUR Project New Methods for Identification and Adaptive Control for Industrial Systems. Recommended by Associate Editor J. Lu.
P. De Filippi, M. Tanelli, M. Corno, and S. M. Savaresi are with the Dipartimento di Elettronica e Informazione, Politecnico di Milano, Milano 20133, Italy (e-mail: defilippi@elet.polimi.it; tanelli@elet.polimi.it; corno@elet.polimi.it; savaresi@elet.polimi.it).
M. D. Santucci is with Piaggio & C. S.p.A., Pontedera 56025, Italy (e-mail: mario.santucci@piaggio.com).

a controlled electronic throttle and an electronically-actuated braking system, which independently acts on the front and rear brakes [23], [24]. The actuator dynamic is explicitly considered in the controller design. The proposed controllers are validated via Bikesim, a multibody motorcycle simulator that considers different challenging maneuvers, such as panic braking on curves and changes in the friction coefficient as well as external disturbances.

II. Analysis of Motorcycle Dynamics

To design a stability control system, one first has to select the most suitable control and controlled variables. In this paper, the inputs that can be manipulated are the torques at the wheels: namely, the traction and braking torque at the rear wheel and the braking torque at the front wheel. Today, drive and brake-by-wire systems are becoming a reality on commercial motorbikes, while active steering systems are not available. To explicitly model the actuator dynamics, we employ low-pass filters with a cut-off frequency of 10 Hz [23], [24].

To enhance the stability of a motorcycle during dangerous maneuvers, one may consider controlling the yaw rate and/or the roll rate of the vehicle. These variables can be measured via MEMS gyroscopes, which are becoming available on board of sport motorcycles as they are employed in advanced traction and braking control systems. Moreover, in order to consider the rider's intention, a longitudinal accelerometer is needed to measure the longitudinal acceleration of the vehicle.

Deriving a control-oriented analytical model of the motorcycle starting from first principles is not trivial; to the best of our knowledge, several multibody models have been derived in [6], [20], [25]–[27]. These models are suitable for simulation and closed-loop validation but too complex for model-based control systems design. In this paper, a black-box approach has been adopted to identify a linearized model of the system dynamics during a steady-state cornering maneuver, using as a basis Bikesim, tuned to fit an sport motorcycle (see [28] for more details on the parameters). Furthermore, to correctly identify the vehicle dynamics of interest, the identification tests have been carried out in open-loop, i.e., without any intervention of the rider.

To identify the linearized model, a steady-state cornering condition has been simulated, with speed $v = 130$km/h and roll angle $\varphi = 30°$; a frequency sweep torque ranging from 0 to 20 Hz has been independently applied to the front and rear wheels. In order to account for the asymmetrical nature of the front wheel torque actuator (only a brake is available) and still apply linear, frequency-based identification techniques, the frequency sweep is applied to the front wheel around a constant negative torque of -5Nm, while for the rear wheel it is applied around the steady-state rear torque (recall that the rear wheel torque can be either positive or negative). Based on the measurement of inputs (i.e., front and rear wheel torques, T_f and T_r) and outputs (i.e., roll rate $\dot{\phi}$, yaw rate $\dot{\psi}$, and longitudinal acceleration a_x), a multi-input-multi-output linear time-invariant model was identified using subspace techniques

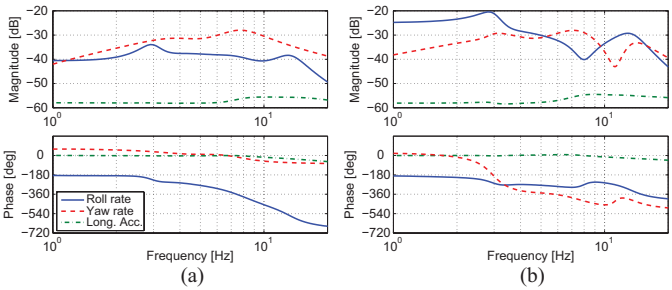

Fig. 1. Magnitude (top) and phase (bottom) Bode diagrams of the frequency response (a) $G_{T_f y}(j\omega)$, and (b) $G_{T_r y}(j\omega)$ $y \in \{\dot{\phi},\ \dot{\psi},\ a_x\}$ for $v = 130$ km/h and $\varphi = 30°$: roll rate (solid line), yaw rate (dashed line), and longitudinal acceleration (dashed-dotted line).

(see [29]). The roll rate is defined with respect to a body fixed reference frame, while the yaw rate is defined with respect to an inertial reference frame. The model is a 7th order system and captures the main out-of-plane dynamics of the motorcycle. The model has been validated with pseudo-random binary inputs for both the front and rear wheel torques, yielding good results and assessing the model suitability for control purposes.

In Fig. 1(a) and (b), the magnitude and phase Bode diagrams of the frequency responses from rear and front wheel torques to the outputs are depicted. The front wheel torque has a greater authority on the roll rate than the rear wheel one, while the front and rear wheel torques have similar influence on the longitudinal acceleration and the yaw rate. Moreover, the principal out-of-plane modes of vibration of the motorcycle are clearly visible. It is worth noticing that all the transfer function models linked to the roll rate and yaw rate show the weave and wobble resonances, typical of the steering dynamics [30], [31], located at approximately 3 and 10 Hz, respectively. Moreover, the magnitude of the frequency response from all the inputs to the longitudinal acceleration is almost constant in the frequency range of interest.

The longitudinal acceleration most naturally controlled by the rider's commands on the gas and brake levers. To enhance the stability, the roll rate and/or the yaw rate could be considered as controlled variable. In what follows, the dynamics from wheel torques to roll rate and yaw rate will be analyzed in order to outline the most favorable controlled variable.

If the longitudinal acceleration and the yaw rate are chosen as controlled variables, the identified model shows one transmission zero in the right half plane at approximately 1.2 Hz that may compromise the performance of the closed-loop system. If, instead, the longitudinal acceleration and the roll rate are considered as controlled variables, the identified model has no transmission zeros in the right half plane and exhibits a real zero at the origin. This is due to the fact that the roll rate is measured in body fixed coordinates and thus the effect of a step variation in the rear or front wheel torque while cornering causes the bike to oscillate and then to stabilize at a different steady-state roll angle with zero roll rate. This analysis shows that the most favorable dynamics are those from front and rear wheel torques to longitudinal acceleration and roll rate. This choice is supported by other

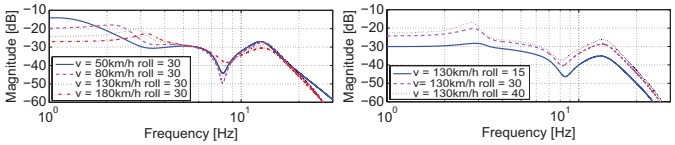

Fig. 2. Magnitude bode diagrams of the frequency response $G_{T_f\dot{\varphi}}(j\omega)$ for different velocities and roll angles.

practical considerations. For example, considering the roll rate φ as output, it is natural to regulate it to zero to prevent falls, while, if the yaw rate is chosen as output, a suitable model has to be derived in order to generate the set-point, which is a difficult problem on its own [5]. Finally, with respect to four-wheeled vehicles, motorcycles are statically unstable and the roll rate is the most natural controlled variable to account for this issue. However, the combined observation of roll-rate and yaw-rate appears to be worth investigation, within a supervisory control framework.

Then, we can conclude that the overall "stability" of the vehicle is increased if the roll rate can be minimized when external disturbances act on the motorcycle. However, it is necessary that the stability controller also regulates the longitudinal acceleration of the vehicle, in order to comply with the rider's intention in terms of acceleration and deceleration.

To analyze how weave and wobble resonances and the overall linearized vehicle dynamics vary in different driving conditions for the considered motorcycle model, a sensitivity analysis of the frequency response $G_{T_f\dot{\varphi}}(j\omega)$ with respect to the steady-state forward speed and roll angle is presented. Fig. 2 depicts the magnitude Bode diagrams of $G_{T_f\dot{\varphi}}(j\omega)$ for different values of v and φ. By inspecting this figure, the following considerations are in order.

1) The wobble mode resonance, located at approximately 13 Hz is nearly invariant to speed and roll angle variations in the considered range. This is consistent with the analysis in [30].
2) The weave mode natural frequency, located in the range 2–4 Hz behaves as follows: for fixed speed, it decreases as the roll angle increases; for fixed roll angle, it increases with speed. Again, this is consistent with previous results [30], [31].
3) The behavior of the (generalized) gain is as follows: for fixed speed, it increases with the roll angle; for fixed roll angle, it decreases as speed increases. A physical explanation of this behavior is not immediate, as acting on the wheel torque while cornering causes a complex interplay between longitudinal and lateral forces due to variations in the wheel slip and in the roll and sideslip angles.

III. Design of an Active Electronic Stability Controller

Once the input and output variables have been defined, we can outline the proposed controller architecture (as shown in Fig. 3). At first, the design of a virtual rider will be presented and then the controller design phase will be addressed, which

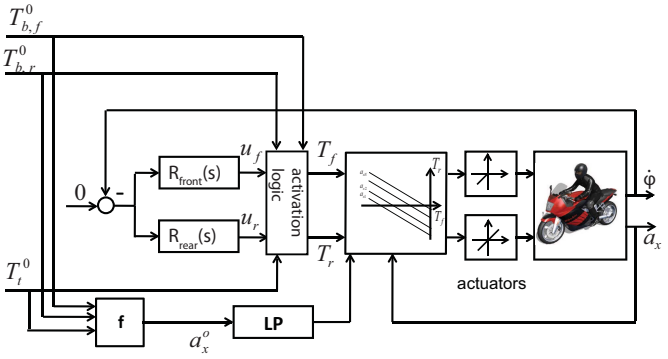

Fig. 3. Block diagram of the closed-loop system regulated by the full-authority saturated controller.

is constituted of two linear and time invariant controllers for the front and rear wheel torque that manage stability, and a saturation block that activates the regulation of the longitudinal acceleration. Finally, the set-point generation for the longitudinal acceleration and the activation and deactivation logic will be discussed.

A. Virtual Rider Design

Motorcycles are statically unstable and the rider plays a critical role in stabilizing the vehicle. This cannot be neglected in the study of a stability control system, and thus a virtual rider has been designed. The rider is modeled as a steering torque controller, neglecting body movements. The driver steering torque is computed as the sum of two terms: a constant term corresponding to the steering torque necessary to keep the initial roll angle, and a feedback term that tracks a zero roll angle rate reference. The constant term is determined beforehand for each condition. The feedback term is generated by a roll rate controller. The controller is designed with classical linear loop-shaping techniques based on the identified steering-torque-to-roll-rate dynamics, achieving a closed-loop bandwidth of 0.5 Hz, compatible with human reaction time [32]. In this application, a fixed structure third order controller has been preferred in order to provide a more immediate comparison among different scenarios

$$R_{\text{driver}}(s) = \frac{5.9\left(s^2 + 5.303s + 366.3\right)}{s\left(s^2 + 11.82s + 512.3\right)}.$$

B. Generation of the Longitudinal Acceleration Set-Point

To comply with the rider's intention and control the longitudinal acceleration accordingly, an appropriate set-point a^0_x must be selected. To this end, the set-point has been scheduled on the basis of the rider's braking and traction request as

$$a^0_x = \alpha_f T^0_{b,f} + \alpha_r T^0_{b,r} + \beta T^0_t + \gamma\,. \tag{1}$$

Equation (1) is to be intended as a reference model for the longitudinal acceleration. The designer has the freedom to choose the most suitable reference model (using more complex, adaptive characteristics). To improve the readability of the results, in what follows, the reference model has been

tuned to match the open-loop acceleration response of the motorcycle during normal operation. It has been identified from simulations where different braking and traction inputs are applied and solving a linear least squares fitting problem.

C. Full Authority Controller With Time-Varying Saturations

If one is interested in controlling the roll rate only, two different controllers can be designed based on the transfer function models $G_{T_r\dot{\varphi}}(s)$ and $G_{T_f\dot{\varphi}}(s)$.

The plant can be represented as a multi-input-single-output system and thus two controllers can be designed: the first controller, the rear-wheel controller, relies only on rear wheel torque actuation (positive and negative); the second controller, the front-wheel controller, actuates only the front wheel braking torque (only negative). A sequential design approach is adopted. At first, the front wheel controller has been designed with classical loop-shaping techniques, yielding a fifth order controller $R_{front}(s)$ that achieves a closed-loop bandwidth of 2.4 Hz with a phase margin of 53.5°.

Then, the rear wheel controller is designed on the resulting closed-loop system $G_{T_r\dot{\varphi}}(s)S_{T_f\dot{\varphi}}(s)$, where

$$S_{T_f\dot{\varphi}}(s) = \frac{1}{1 + R_{\text{front}}(s)G_{T_f\dot{\varphi}}(s)}$$

is the sensitivity function of the front wheel control loop and $G_{T_r\dot{\varphi}}(s)$ is the linearized transfer function model from the rear wheel torque to the roll rate. The design procedure yields the sixth order controller $R_{\text{rear}}(s)$ that achieves a closed-loop bandwidth of 1.5 Hz and a phase margin of 68.9°. The sequential design started with the front wheel controller because the open-loop dynamics are more favorable and thus a larger bandwidth can be achieved. Note that the control variables u_f and u_r are added to the rider's front and rear braking ($T^0_{b,f}$ and $T^0_{b,r}$) and traction (T°_t) requests, to yield

$$T_r = u_r + T^0_t + T^0_{b,r}, \quad T_f = u_f + T^0_{b,f}. \tag{2}$$

Such a controller makes the best use of the available actuation to restore the stability of the motorcycle: it takes advantage of the good dynamic response of the front wheel torque and, thanks to the intervention of the rear torque, it circumvents the limitation due to the fact that only negative torques can be applied to the front wheel. However, it does not comply with the rider's acceleration and deceleration commands as the longitudinal acceleration of the motorcycle is not regulated. To do this, a time-varying saturation block scheduled on the desired longitudinal acceleration a^0_x has been designed.[1] A saturation of the rear wheel torque intervenes only if the absolute value of the vehicle longitudinal acceleration exceeds the low-pass filtered set-point value. The time-varying saturation is derived from (1), namely, the rear wheel torque is set to the value that guarantees the desired longitudinal acceleration considering the current torque that is being applied to the front wheel. This guarantees that the front torque, which is more effective in controlling the roll rate, is left free whereas the rear torque is used to control the longitudinal acceleration. If the current longitudinal acceleration is lower than the requested then both torques are employed to stabilize the roll dynamics. Clearly, with such a complex saturation strategy, the proof of the closed-loop system stability is not trivial. Current research is being focused on this topic.

Fig. 3 depicts a schematic view of this control system. In the following, this control architecture will be referred to as full-authority controller with time-varying saturations (FA-SAT).

D. Activation and Deactivation Logic

Once the control system has been designed, an activation and deactivation logic must be implemented to ensure that the control system intervenes only when facing dangerous situations.

In Fig. 4, the block diagram of the activation and deactivation logic is depicted. In normal operation, the controller is off and therefore the front (rear) wheel torque is the one requested by the rider. If a dangerous situation is detected, the controller is turned on ($\text{act}_i = 1,\ i = f, r$) and the wheel torques are computed as

$$T_f = T^0_{b,f} + u_f = T_{d,f} + u_f,\ T_r = T^0_{b,r} + T^0_t + u_r = T_{d,r} + u_r$$

where $T_{d,f} = T^0_{b,f}$ and $T_{d,r} = T^0_{b,r} + T^0_t$ are the requested front and rear wheel torque.

Once the vehicle has been stabilized, the deactivation phase starts ($dct_i = 1,\ i = f, r$). Let $\overline{u}_i,\ i = f, r$ be the values of the control variables at the beginning of the deactivation phase, and $u_{i,\text{LP}},\ i = f, r$ a low-pass filtered version of $\overline{u}_i$ with a cut-off frequency of 0.5 Hz. The LP filter is initialized at zero when dct is triggered. As the front wheel torque has a greater authority on the roll rate, to avoid oscillations during the deactivation phase, a third-order low-pass filter is used for the front wheel torque and a first-order one for the rear wheel torque. When the LP filters are at steady-state, say for $t \geq t^*$, $u_{i,\text{LP}}(t) = \overline{u}_i$ and $T_i(t) = T_{d,i}\ \forall t \geq t^*$. During the deactivation phase, the filtered version of the last value of the control variable $\overline{u}_i$ is subtracted from the rider's torque request and from the control variable itself. Thus, the front-wheel controller or the rear-wheel controller is turned off when the front or rear wheel torque is equal to the value requested by the rider, respectively. Then, the deactivation can be completed by letting $\overline{u}_i(t) = 0,\ u_{i,\text{LP}}(t) = 0,\ t > t^*$. This ensures that a smooth transient is experienced while returning full control to the rider.

A finite state machine (FSM) activates and deactivates the control system (see Fig. 4). The control system is activated when $\ddot{\varphi} \geq \ddot{\varphi}_{\text{th}}$ where $\ddot{\varphi}$ is the roll acceleration obtained by properly filtering the roll rate $\dot{\varphi}$ and where $\ddot{\varphi}_{\text{th}}$ is a user-defined threshold. Thus, if condition (III-D) holds, the FSM sets the activation flags $\text{act}_{f,r}$ to one. The controller is deactivated when $P_{\ddot{\varphi}} \leq P_{\text{th}}$,where P_{th} is a user-defined threshold and

$$P_{\ddot{\varphi}} = \frac{1}{T}\int_{t-T}^{t} \ddot{\varphi}^2(\tau)d\tau \tag{3}$$

is the power of the roll acceleration signal, where $T = 0.5$ s has been experimentally selected. Note that in this approach,

[1]To decouple the roll rate control loop from the acceleration-based saturations, a low-pass filter is needed.

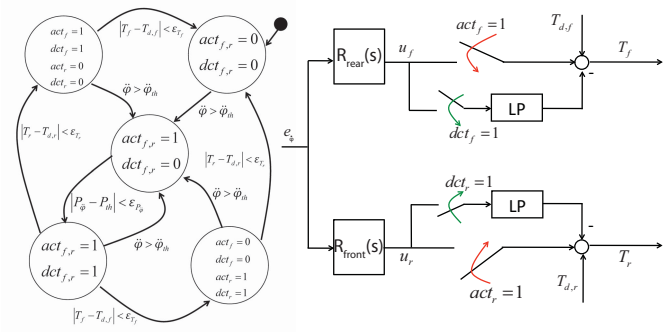

Fig. 4. Schematic view of the activation finite state machine and the activation and deactivation logic.

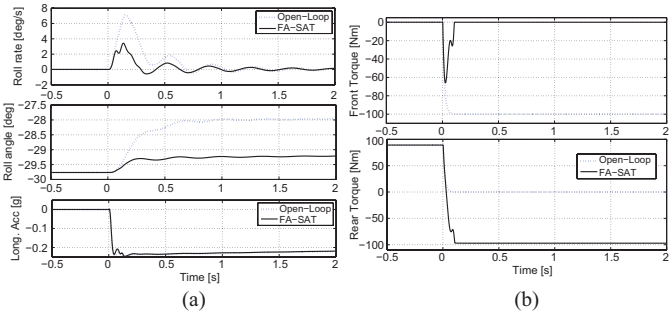

Fig. 5. Time histories of (a) roll rate (top), roll angle (middle), and longitudinal acceleration (bottom), and (b) front (top) and rear (bottom) wheel torque in response to a 100 Nm disturbances on the braking torque of the front wheel.

thresholds $\ddot{\varphi}_{\text{th}}$ and P_{th} can be tuned to render the control system more or less intrusive. Finally, when both controllers are deactivated ($dct_{f,r} = 0$), the control system is definitely turned off and the rider has full control of the vehicle.

Remark 3.1: Note that an unnecessary activation does not compromise the stability of the vehicle. In fact, the motorcycle may result less smooth to ride on turns due to the limitations on the roll rate but the rider will able to perform all the maneuvers. On the other hand, if the activation and deactivation logic does not recognize a dangerous situation, the vehicle behaves as a standard motorcycle. Thus, also in this case, the control system does not compromise rideability introducing additional safety hazards.

IV. Validation of the Active Stability Controller

The current section is devoted to the validation of the proposed control strategy. Validation is performed via simulations in Bikesim. The controller is tested in different critical conditions, designed to excite the bike with perturbations on the wheel torques and on the road surface. Specifically, the following three different conditions are analyzed:

1) front wheel braking while cornering (panic braking on curve);
2) double step variation of the tire/road friction coefficient while braking on a curve (μ-jump);
3) force disturbance applied to the rider's saddle.

All simulations are performed at an initial constant forward speed $v = 130$ km/h with roll angle $\varphi = -30°$, namely, the values considered during controller tuning. In order to evaluate the performance of the stability controllers, all tests have been carried out with the controllers always active. A discussion on the performance modifications due to the activation and deactivation logic that will be tested in the presence of measurement noise, will be presented in a dedicated remark.

A stability control system is expected to prevent falls when the rider is not able to stabilize the vehicle in open-loop, i.e., without any electronic control system. This scenario is not ideal for analyzing the features of the control system as it would make comparison possible only in a binary sense—either the maneuver fails or not—thus hiding several subtleties. To clearly present these features, the validation of the controllers has been carried out by progressively increasing the amplitude of the perturbation signal so as to reach the limiting conditions before a fall occurs. A dedicated remark will discuss the performance of the controllers when the rider loses control of the vehicle.

To quantitatively evaluate the performance of the control systems, the root-mean-square (RMS) of the roll rate (recall that a zero set-point was selected for the roll rate) and the RMS of the difference between the acceleration a_x achieved in closed-loop and that (a_x^{OL}) measured in open-loop have been introduced, thus yielding the following cost functions:

$$J_{\dot{\varphi}} = \sqrt{\frac{1}{N}\sum_{k=1}^{N}\dot{\varphi}(k)^2}, \quad J_{a_x} = \sqrt{\frac{1}{N}\sum_{k=1}^{N}\left(a_x(k) - a_x^{OL}(k)\right)^2} \tag{4}$$

where N is the number of samples considered to compute the cost functions. The first cost function measures the vehicle stability, while the second evaluates the driver's feeling in terms of rideability. Both cost functions are computed starting from the time instant when the perturbation is applied and they penalize both the amplitude of the oscillations and the settling time.

A. Front Wheel Braking Torque Disturbance

The first test simulates a rider braking during high speed cornering. This is a critical situation because, as the longitudinal tire force is increased, the lateral force decreases, yielding reduced grip and limited maneuverability. This condition has been simulated imposing a negative step variation of both front and rear wheel torque, namely, the rider closes the throttle and acts on the front brake lever to decrease the forward speed while cornering.

Fig. 5 depicts the time histories of the roll rate, roll angle, and longitudinal acceleration in open-loop and with the FA-SAT controller. A front braking torque input of -100 Nm with a sudden closing of the throttle (i.e., T_r is set to zero with a 10-Hz low-pass filtered dynamics that account for the effect of the actuator) is simulated.

By inspecting Fig. 5, the following conclusions can be drawn.

1) As soon as the rider's inputs are applied, the roll rate increases and the motorcycle tends to reduce its roll angle. This is due to the velocity decrease caused by braking.
2) In the open-loop case, the rider takes more than one second to stabilize the vehicle around the new

TABLE I

VALUES OF THE COST FUNCTIONS FOR DIFFERENT FRONT BRAKING TORQUE DISTURBANCES RANGING FROM -10 TO -200 nm

T_{bf} [Nm]		-50	-100	-150	-200
$J_{\dot{\varphi}}$	Openloop	1.04	1.77	2.45	3.09
	FA-SAT	0.445	0.709	0.996	1.29
$J_{a_x}[\cdot 10^{-4}]$	FA-SAT	13	31	57	95.1

steady-state roll angle and considerable weave oscillations are observed.

3) The active stability controller improves the responses both in terms of settling time and amplitude of weave oscillations.
4) The final steady roll angle obtained in the FA-SAT case is only 0.5° away from the initial angle, while in the open-loop case, the motorcycle looses more than 1.5°.
5) The deceleration achieved by the FA-SAT controller is very close to the one obtained in open-loop.

In Fig. 5(b), the front and rear wheel torques are depicted. As can be seen, after approximately 100ms both the front and rear wheel torques are saturated to follow the acceleration set-point. The FA-SAT controller guarantees good performance both for the roll rate and the longitudinal acceleration of the motorcycle. It is worth noticing that, in this test, the controllers act as an electronic brake distribution (EBD) system that splits up the needed braking torque to the rear and front wheel in order to minimize the effects of the disturbances.

To better appreciate the performance of the active stability controller, in Table I the values of the cost functions as a function of the amplitude of the front wheel braking torque disturbance are depicted. The closed-loop strategies always improve the stability of the vehicle. Analyzing the roll rate cost function, an improvement between 40% and 60% with respect to the open-loop case is achieved, and the FA-SAT controller guarantees a longitudinal acceleration very close to the one obtained in open-loop, thus not compromising the natural feeling of the motorcycle.

Remark 4.1 (Open-Loop Fall): As previously discussed, the stability control system should stabilize the motorcycle even when the rider in open-loop is not able to control the vehicle and falls. Fig. 6 depicts the performance obtained in open-loop and with the FA-SAT controller when a step input of the front braking torque of 300 Nm is simulated. As can be seen, the FA-SAT controller stabilizes the motorcycle, while the rider loses the control of the motorcycle. This test shows that the stability controller is indeed crucial for enhancing active safety.

Remark 4.2 (Activation Logic): To evaluate the performance modifications due to the activation and deactivation logic, several simulation tests have been performed. Fig. 7 presents a comparison between the open-loop case, the FA-SAT ideal case (without activation logic), and the FA-SAT realistic case with activation logic and measurement noise. The noise has been taken from an actual, industrial roll rate sensor [33]. In the FA-SAT realistic case, a slight loss of

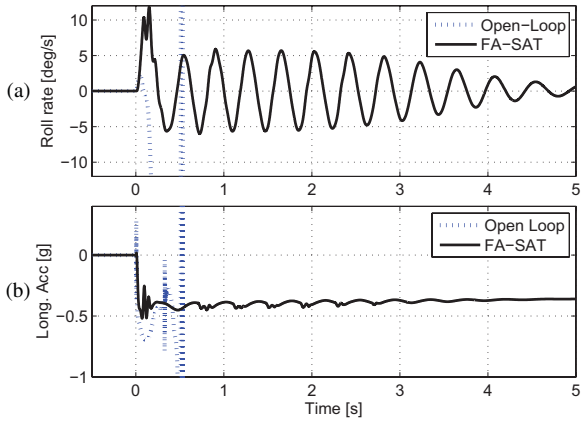

Fig. 6. Time histories of the roll rate (top) and the longitudinal acceleration (bottom) in response to a 300-Nm disturbance on the braking torque of the front wheel.

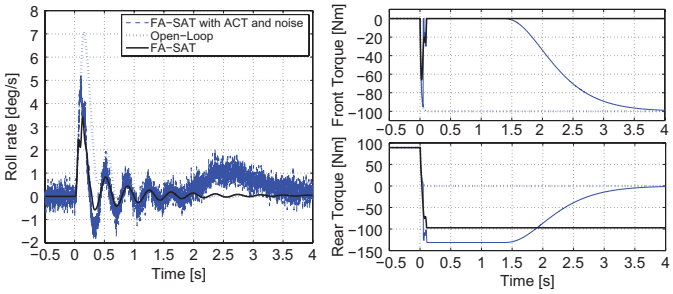

Fig. 7. Time histories of the roll rate in response to a 100-Nm disturbance on the braking torque of the front wheel when the activation and deactivation logic is implemented: open-loop (dotted line), FA-SAT (solid line), and FA-SAT controller with activation and deactivation logic and measurement noise (dashed line).

performance can be noted in the first part of the transient response. As expected, the attenuation of the first peak is worse than the one obtained in the ideal case. This is due to the activation delay due to the FSM. Moreover, a very low frequency oscillation can be noted when the control system is deactivated. This oscillation is not critical as it is at a very low frequency and of small amplitude, so that the rider can easily control it. It is interesting to note that the proposed logic is also robust to noise. The threshold-based actuation is not sensitive to noise (the roll rate acceleration caused by the disturbance is clearly detectable) and the reduced bandwidth of the wheel torque controller guarantees a smooth control action. Therefore, the responses can be considered satisfactory even if the activation and deactivation logic is implemented in a noisy environment. By inspecting the front and rear wheel torques in Fig. 7, it can be noted that after 1.5 s the deactivation phases start and at the end of the transient response, the wheel torques are equal to those requested by the rider.

Remark 4.3 (Riding Feeling): Another variable that quantifies the stability as perceived by the rider is the steering angular rate $\dot{\delta}$. To give a quantitative measure of this aspect, the RMS of the steering angular rate has been introduced

$$J_{\dot{\delta}} = \sqrt{\frac{1}{N}\sum_{k=1}^{N}\dot{\delta}(k)^2}. \tag{5}$$

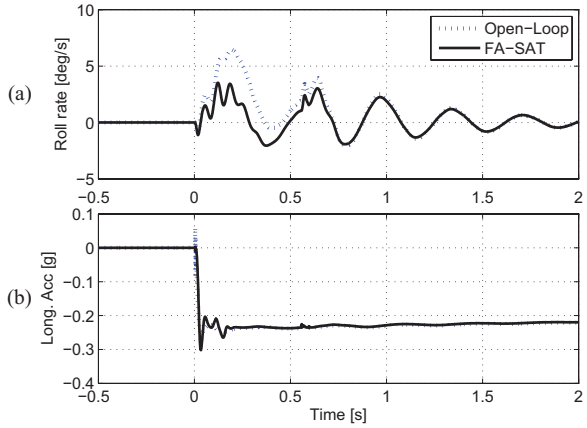

Fig. 8. Time histories of the roll rate (top) and the longitudinal acceleration (bottom) in response to a 100-Nm disturbances on the braking torque of the front wheel and a sudden change in the tire/road friction coefficient ($L = 20$ m).

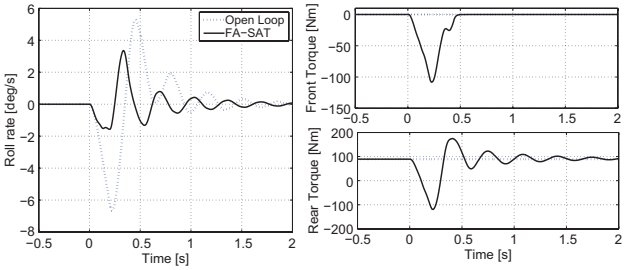

Fig. 9. Time histories of the roll rate and control torques as a response to a 60-N lateral force impulse applied at the saddle.

In simulations of the panic braking maneuver, a value of $J_{\dot{\delta}} = 0.78$ for the FA-SAT case is found that is to be compared to $J_{\dot{\delta}} = 0.616$ for the open-loop case. The difference is inverted when the contribution in the frequency range 0–3 Hz is considered: $J_{\dot{\delta}} = 0.18$ against $J_{\dot{\delta}} = 0.295$ of the open loop case. The range 0–3 Hz is the frequency range where the rider is most sensitive. It can be concluded that the controller improves the damping of the oscillations within the rider's bandwidth, or more precisely it shifts the steering variation more toward high frequency where are less disruptive.

Remark 4.4 (Analysis of Different Maneuvers): To further test the closed-loop performance, two other maneuvers are considered: the so-called μ-jump test and a force disturbance applied to the saddle. For the μ-jump, a sudden change of the tire/road friction coefficient is simulated while braking. A positive, i.e., from $\mu = 0.7$ to $\mu = 1$ and then back to $\mu = 0.7$, and negative, i.e., from $\mu = 0.7$ to $\mu = 0.5$ and then back to $\mu = 0.7$, variation of the tire/road friction coefficient has been considered. Another maneuver is discussed in details in [22]).

Fig. 8 shows the time-histories of the roll rate and of the longitudinal acceleration for a positive variation of the tire/road friction coefficient when a front braking disturbance of -100 Nm and a sudden closing of the throttle are simulated. The length of the road section is $\Delta L = 20$ m. The considerations outlined previously still hold. It is interesting to notice that, at approximately $t = 0.570$ s, the roll rate is subject to a second disturbance: this is due to the fact that the front tire passes over the second transition of tire/road friction coefficient.

Several simulations have been carried out considering different lengths of the high friction road section. The performance is consistent: an improvement in the roll rate cost function (4) between 36% and 57% with respect to the open-loop case is achieved. Similar results have been obtained on a road section with reduced friction.

Another interesting point of view is the evaluation of the capability of the controller to stabilize the motorcycle when affected by a disturbance that is not co-located with the control action, namely, it does not come from the tire/road interaction. To test this scenario, a lateral force is applied to the saddle. Fig. 9 shows the results when a triangular impulse of 60 N is applied. Also in this case, the control system is capable of rejecting the disturbance and considerably reducing the oscillations with respect to the open-loop case.

Remark 4.5 (Sensitivity to the Working Condition): As discussed in Section II, the damping and natural frequency of weave and wobble modes depends on the forward speed and the roll angle (see also [20], [25], [31], [34]). Thus, it is interesting to evaluate the performance of the stability control systems in different working conditions. For sake of brevity, only the front wheel braking disturbance case is considered. Similar results have been obtained for the other maneuvers. Note that the forward speed value of 80km/h has been chosen so as to be below the critical velocity for the considered motorcycle model, which is the velocity value above which the rider needs to counter-steer to successfully perform a turn, [20].

In Table II, the values of the cost function (4) for different initial velocity and roll angle are collected. First, notice that at $v = 180$ km/h, the motorcycle is not capable of negotiating the corner with $\varphi = 45°$ and thus this condition is not considered in the discussion. As expected, in general, the control system performs better around the conditions in which it has designed (expect for the $v = 180$ km/h, $\varphi = 45°$ case). The performance clearly depends on the velocity; this is due to the fact that the weave mode cancellation performed by the controller is approximate for speed values different from the design one. On the other hand, for velocities lower or equal to the design one the larger the roll angle, the better the performance achieved with the closed-loop systems. This is due to the fact that for large roll angles, the in-plane and out-of-plane dynamics are coupled and thus the control action is more effective. This does not hold at high speed because the $\varphi = 30°$ case is close to the adhesion limits of the tires. As the spread of the cost function (4) is limited, it can be concluded that this loss of performance is acceptable. However, in order to guarantee the same performance over the whole range of forward speed and roll angles, a gain-scheduled solution needs to be devised.

Finally, an analysis aimed at studying the effects of different actuator bandwidths has been carried out. The analysis underlines that reducing the actuators bandwidth to 2 Hz only marginally affects performance (1%).

TABLE II

VALUES OF THE COST FUNCTION (4) FOR DIFFERENT INITIAL SPEED AND INITIAL ROLL ANGLE

Control	$v = 80$km/h			$v = 130$km/h			$v = 180$km/h		
Strategy	$\varphi = 15°$	$\varphi = 30°$	$\varphi = 45°$	$\varphi = 15°$	$\varphi = 30°$	$\varphi = 45°$	$\varphi = 15°$	$\varphi = 30°$	$\varphi = 45°$
FA-SAT	54%	45%	40%	49%	40%	35%	41%	54%	N.A.

V. CONCLUSION

In this paper, the problem of designing an electronic stability control system for PTW's was addressed. A control architecture that first recovers stability and then ensures that the longitudinal acceleration requested by the rider is followed was presented, which is endowed with an activation and deactivation logic. The robustness of the control systems with respect to different maneuvers, different working conditions, and measurement noise was investigated, yielding promising results. Current research is being devoted to the experimental validation of the control strategies.

ACKNOWLEDGMENT

The authors would like to thank L. Fabbri for the stimulating discussions.

REFERENCES

[1] S. M. Savaresi and M. Tanelli, *Active Braking Control Systems Design Vehicles*. New York: Springer-Verlag, 2010.

[2] F. Borrelli, A. Bemporad, M. Fodor, and D. Hrovat, "An MPC/hybrid system approach to traction control," *IEEE Trans. Control Syst. Technol.*, vol. 14, no. 3, pp. 541–552, May 2006.

[3] M. Canale, L. Fagiano, A. Ferrara, and C. Vecchio, "Comparing internal model control and sliding-mode approaches for vehicle yaw control," *IEEE Trans. Intell. Transp. Syst.*, vol. 10, no. 1, pp. 31–41, Feb. 2009.

[4] M. Abe, Y. Kano, K. Suzuki, Y. Shibahata, and Y. Furukawa, "Side-slip control to stabilize vehicle lateral motion by direct yaw moment," *Japanese Soc. Autom. Eng. Rev.*, vol. 22, no. 4, pp. 413–419, Oct. 2001.

[5] M. Canale, L. Fagiano, M. Milanese, and P. Borodani, "Robust vehicle yaw control using an active differential and IMC techniques," *Control Eng. Pract.*, vol. 15, no. 8, pp. 923–941, 2007.

[6] D. J. N. Limebeer, R. S. Sharp, and S. Evangelou, "The stability of motorcycles under acceleration and braking," in *Proc. Inst. Mech. Eng., C, J. Mech. Eng. Sci.*, vol. 215, no. 9, pp. 1095–1109, Sep. 2001.

[7] V. Cossalter, R. Lot, and F. Maggio, "On the stability of motorcycle during braking," in *Proc. SAE Small Engine Technol. Conf. Exhibit.*, Sep. 2004, pp. 1–15.

[8] S. M. Savaresi, M. Corno, S. Formentin, and L. Fabbri, "System and method for controlling traction in a two-wheeled vehicle," U.S. Patent 0312449, Dec. 15, 2010.

[9] T. Kazuhiko, N. Yutaka, N. Takehiko, T. Kazuya, and T. Makoto, "Control technologies of brake-by-wire system for super-sport motorcycles," in *Proc. SAE World Congr. Exhibit.*, Apr. 2010, no. 2010-01-0080, DOI: 10.4271/2010-01-0080.

[10] T. Wakabayashi and K. Sakai, "Development of electronically controlled hydraulic rotary steering damper for motorcycles," in *Proc. 5th Int. Motorcycle Safety Conf.*, 2004, pp. 490–509.

[11] M. Tanelli, C. Vecchio, M. Corno, A. Ferrara, and S. M. Savaresi, "Traction control for ride-by-wire sport motorcycles: A second order sliding mode approach," *IEEE Trans. Ind. Electron.*, vol. 56, no. 9, pp. 3347–3356, Sep. 2009.

[12] P. Cardinale, C. D'Angelo, and M. Conti, "Traction control system for motorcycles," *EURASIP J. Embedded Syst.*, vol. 2009, no. 3, pp. 393–438, 2009.

[13] M. Tanelli, M. Corno, I. Boniolo, and S. M. Savaresi, "Active braking control of two-wheeled vehicles on curves," *Int. J. Veh. Auto. Syt.*, vol. 7, nos. 3–4, pp. 243–269, 2010.

[14] M. Corno, S. M. Savaresi, and G. J. Balas, "On linear parameter varying (LPV) slip-controller design for two-wheeled vehicles," *Int. J. Robust Nonlinear Control*, vol. 19, no. 12, pp. 1313–1336, Aug. 2009.

[15] P. De Filippi, M. Tanelli, M. Corno, S. M. Savaresi, and L. Fabbri, "Semi-active steering damper control in two-wheeled vehicles," *IEEE Trans. Control Syst. Technol.*, vol. 19, no. 5, pp. 1003–1020, Sep. 2011.

[16] P. De Filippi and S. M. Savaresi, "A mixed frequency/time-domain method to evaluate the performance of semi-active steering damper control strategies during challenging maneuvers," in *Proc. 11th ASME Dyn. Syst. Control Conf.*, Arlington, Oct.–Nov. 2011, pp. 815–822.

[17] S. A. Evangelou, D. J. N. Limebeer, and M. Tomas-Rodriguez, "Suppression of burst oscillations in racing motorcycles," in *Proc. 49th IEEE Conf. Decision Control*, Dec. 2010, pp. 5578–5585.

[18] S. A. Evangelou, "Control of motorcycles by variable geometry rear suspension," in *Proc. IEEE Int. Conf. Control Appl.*, Sep. 2010, pp. 148–154.

[19] J. Yi, Y. Zhang, and D. Song, "Autonomous motorcycles for agile maneuvers, part II: Control system design," in *Proc. 48th IEEE Conf. Decision Control*, Dec. 2009, pp. 4619–4624.

[20] V. Cossalter, *Motorcycle Dynamics*. Orlando, FL: Harcourt Brace Jovanovich, 2002.

[21] P. De Filippi, M. Tanelli, M. Corno, and S. M. Savaresi, "Towards electronic stability control for two-wheeled vehicles: A preliminary study," in *Proc. 10th ASME Dyn. Syst. Control Conf.*, Sep. 2010, pp. 133–140.

[22] P. De Filippi, M. Tanelli, M. Corno, and S. M. Savaresi, "Enhancing active safety of two-wheeled vehicles via electronic stability control," in *Proc. 18th IFAC World Congr. Autom. Control*, 2011, pp. 638–643.

[23] M. Corno, M. Tanelli, S. M. Savaresi, and L. Fabbri, "Design and validation of a gain-scheduled controller for the electronic throttle body in ride-by-wire racing motorcycles," *IEEE Trans. Control Syst. Technol.*, vol. 19, no. 1, pp. 18–30, Jan. 2011.

[24] A. Dardanelli, G. Alli, and S. M. Savaresi, "Modeling and control of an electro-mechanical brake-by-wire actuator for a sport motorbike," in *Proc. 5th IFAC Symp. Mech. Syst.*, 2010, pp. 524–531.

[25] D. J. N. Limebeer, R. S. Sharp, and S. Evangelou, "Motorcycle steering oscillations due to road profiling," *J. Appl. Mech.*, vol. 69, no. 6, pp. 724–739, 2002.

[26] V. Cossalter and R. Lot, "A motorcycle multi-body model for real time simulations based on the natural coordinates approach," *Veh. Syst. Dynamics, Int. J. Veh. Mech. Mobility*, vol. 37, no. 6, pp. 423–447, 2002.

[27] R. S. Sharp, S. Evangelou, and D. J. N. Limebeer, "Advances in the modelling of motorcycle dynamics," *Multibody Syst. Dyn.*, vol. 12, no. 3, pp. 251–283, Sep. 2004.

[28] M. Corno, S. M. Savaresi, M. Tanelli, and L. Fabbri, "On optimal motorcycle braking," *Control Eng. Pract.*, vol. 16, no. 6, pp. 644–657, 2008.

[29] P. van Overschee and B. DeMoor, *Subspace Identificatation of Linear Systems: Theory, Implementation, Application*. Norwell, MA: Kluwer, 1996.

[30] S. Evangelou, D. J. N. Limebeer, R. S. Sharp, and M. C. Smith, "Control of motorcycle steering instabilities," *IEEE Control Syst. Mag.*, vol. 26, no. 5, pp. 78–88, Oct. 2006.

[31] M. Tanelli, M. Corno, P. De Filippi, S. Rossi, S. M. Savaresi, and L. Fabbri, "Control-oriented steering dynamics analysis in sport motorcycles: Modeling, identification and experiments," in *Proc. 15th IFAC Symp. Mach. Syst. Identificat.*, 2009, pp. 468–473.

[32] R. Lot, M. Massaro, and R. Sartori, "Advanced motorcycle virtual rider," *Veh. Syst. Dyn.*, vol. 46, no. 1, pp. 215–224, 2008.

[33] I. Boniolo and S. M. Savaresi, *Estimate of the Lean Angle of Motorcycles*. New York: VDM Verlag, 2010.

[34] R. S. Sharp and D. J. N. Limebeer, "On steering wobble oscillations of motorcycles," *Proc. Inst. Mech. Eng., C, J. Mech. Eng. Sci.*, vol. 218, no. 12, pp. 1449–1456, 2004.

[35] S. M. Savaresi, P. De Filippi, M. Tanelli, M. Corno, and L. Fabbri, "System and method for the active stability control of two-wheeled vehicles," U.S. Patent A 000 980, Dec. 5, 2011.